Dyes and Pigments 92 (2012) 1376–1383

Contents lists available at SciVerse ScienceDirect

Dyes and Pigments

journal homepage: www.elsevier.com/locate/dyepig

Binding of the phenothiazinium dye methylene blue with single stranded polyriboadenylic acid

Maidul Hossain, Ayesha Kabir, Gopinatha Suresh Kumar*

Biophysical Chemistry Laboratory, CSIR-Indian Institute of Chemical Biology, 4, Raja S.C. Mullick Road, Kolkata 700 032, India

ARTICLE INFO

Article history:
Received 22 June 2011
Received in revised form
14 September 2011
Accepted 22 September 2011
Available online 1 October 2011

Keywords:
Phenothiazinium dye
Methylene blue
Poly(A) binding
Self-assembly
Spectroscopy
Calorimetry

ABSTRACT

The binding of the phenothiazinium dye methylene blue to single stranded poly(riboadenylic acid) was investigated by spectroscopic and calorimetric techniques. The binding was cooperative and the affinity was of the order of 10^6 M^{-1} at 100 mM [Na^+] as determined from absorbance, fluorescence and calorimetric studies. Ferrocyanide quenching studies showed intercalative binding of methylene blue to poly(riboadenylic acid). The binding perturbed the circular dichroism spectrum of poly(riboadenylic acid) with concomitant formation of prominent exciton split type of extrinsic CD bands in the 550–700 nm region. The interaction involved a single binding mode with a 1:2 binding stoichiometry. The binding affinity increased with [Na^+] ion concentration in the range 10–200 mM [Na^+]. Dye binding induced self-assembled duplex formation in poly(riboadenylic acid). The biological utility of the dye methylene blue in probing nucleic acid structure is revealed from these studies.

1. Introduction

Studies on the interaction of many dyes with nucleic acids have been of great interest for understanding the molecular aspects of the interaction on one hand and to develop better therapeutic agents for photodynamic therapy on the other. Methylene blue (MB) (3,7-bis(dimethylamino)-phenothiazin-5-ium chloride) (Fig. 1) is one of the most extensively studied dyes for its intercalative interaction with DNA [1–6]. MB, belonging to the phenothiazinium group, is a photosensitizer that has been extensively used as an optical probe in many biochemical systems [7–10]. MB also generates singlet oxygen ($^1O_2$) in presence of oxygen and light [11] The interaction of methylene blue results in oxidative DNA damage producing mostly guanine base modifications resulting in 7,8-dihydro-8-oxoguanine (8-oxoG) and other minor nucleotide modifications [11,12]. The administration of MB for various applications has been approved by the Federal Drug and Food Administration (FDA). Although double stranded DNA binding aspects of MB have been clearly revealed, studies with single stranded DNA and RNA conformations are scarce [13]. In the last few years there has been a significant shift to study and understand the fundamentals of small molecule interactions with various RNA structures in order to develop RNA targeted therapeutic agents [14–16].

Polyriboadenylic acid [poly(A)] has been the focus of attention for its importance in mRNA functioning [17,18]. All eukaryotic mRNAs have a long poly(A) tail at the 3′-end that is an important determinant in its maturation and stability, and in the initiation of translation. Molecules that can bind to the polyadenylate tail may inhibit mRNA function and impair protein production in the cell. This switching off of the protein production by targeting poly(A) tail may be a new route for the development for RNA based therapeutic agents.

Polyriboadenylic acid has the unique characteristics to exist either as a single stranded helix or as a parallel stranded double helical structure. These structures have been fully characterized [19–21], the latter being stabilized by base paired protonated adenines. Many small molecules, particularly alkaloids, have been shown to induce a unique self-assembled structure formation in poly(A), similar to the low pH induced bihelix, the mechanism of which is still obscure [15,16,22,23]. Furthermore, the possibility of double stranded poly(A) formation in the cell leading to the arrest of protein production has not been excluded [24,25]. Apparently, molecules that could induce self-assembly in single stranded poly(A) may be useful as potential lead compounds for controlling the poly(A) chain elongation leading to mRNA degradation. To understand the molecular basis of self-assembled structure formation in

* Corresponding author. Tel.: +91 33 2499 5723/2472 4049; fax: +91 33 2473 5197/2472 3967.
E-mail addresses: gskumar@csiriicb.in, gsk.iicb@gmail.com, gskumar@iicb.res.in (G. Suresh Kumar).

0143-7208/$ – see front matter © 2011 Elsevier Ltd. All rights reserved.
doi:10.1016/j.dyepig.2011.09.016

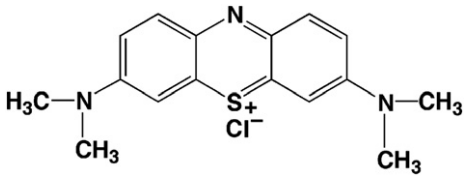

Fig. 1. Chemical structure of methylene blue.

single stranded poly(A), the binding aspects of more complex molecules needs to be investigated. Toward this goal, in this study, we investigated the DNA intercalating photosensitizer dye and FDA approved drug methylene blue interaction with single stranded polyriboadenylic acid structure.

2. Materials and methods

2.1. Materials

Methylene blue (MB) (>95% pure), a product of Riedel-de Haen, GmBH, was obtained from Sigma–Aldrich GmBH. The dye was recrystallized twice from methanol containing hydrochloric acid to yield the hydrochloride salt. Polyriboadenylic acid as potassium salt was a product from Sigma–Aldrich Corporation (St. Louis, MO, USA). Concentration of poly(A) in terms of nucleotide phosphate was determined by UV absorbance measurements at 257 nm using molar extinction coefficient (ε) values of 10,000 M^{-1} cm^{-1} [26]. All the studies were performed in Citrate–Phosphate (CP) buffer, pH 7.0 containing 5 mM of disodium hydrogen phosphate and 0.75 mM of citric acid. Salt dependent studies were performed in the same buffer containing different [Na^+] ions. Analytical grade reagents and deionized and triple distilled water were used all throughout.

2.2. Preparation of dye solutions

Stock solutions of MB were prepared in the experimental buffer and kept protected in the dark till use to avoid any light induced photochemical changes. The dye obeyed Beers' law in the concentration range used in this study. The concentration of MB was determined by absorbance measurements using a molar extinction coefficient (ε) value of 76, 000 M^{-1} cm^{-1} at 664 nm [5]. The purity of the dye solution was checked by measuring the ratio of the absorbance at 665 nm to that at 610 nm, which was always greater than 2.1 indicating the absence of any demethylated dye in the sample [27].

2.3. Absorption titration experiments

The absorption spectral titrations were performed under constant stirring at 20 ± 0.5 °C on a Jasco V660 unit (Jasco International Co. Ltd., Hachioji, Japan) equipped with a thermoelectrically controlled cell holder and temperature controller in matched quartz cuvettes of 1 cm path length (Hellma, Germany), following generally the methods standardized in our laboratory and described earlier [28].

2.4. Analysis of binding data and evaluation of binding parameters

The spectral changes observed in absorption measurements were used to calculate the intrinsic binding constants using Scatchard plots of r/C_f versus r that were further analyzed using the neighbor exclusion model of McGhee–von Hippel [29], as per the following equation

$$\frac{r}{C_f} = K_i(1-nr) \times \left(\frac{(2\omega+1)(1-nr)+(r-R)}{2(\omega-1)(1-nr)}\right)^{(n-1)} \left(\frac{1-(n+1)r+R}{2(1-nr)}\right)^2 \quad (1)$$

where, $R = \{[1-(n+1)r]^2 + 4\omega r(1-nr)\}^{1/2}$, K_i is the intrinsic binding constant to an isolated binding site, n is the number of base pairs excluded by the binding of a single ligand molecule and ω is the cooperativity factor. The binding data were analyzed using the Origin 7.0 software (Origin Labs, Northampton, MA, USA) that determines the best-fit parameters to equation (1).

2.5. Fluorescence studies

Steady state fluorescence spectral measurements were performed on a Hitachi-F4010 fluorescence spectrometer (Hitachi Ltd., Tokyo, Japan) in fluorescence free quartz cuvettes of 1 cm path length as described previously [30]. The excitation wavelength for methylene blue was 610 nm and the emission intensity was monitored in the range 625–750 nm keeping an excitation and emission band pass of 5 nm. The sample cell was thermostated using an Eyela Unicool water bath (Tokyo Rikakikai, Tokyo, Japan) and all the measurements were performed at 20 ± 0.5 °C under conditions of constant stirring. Uncorrected fluorescence spectra were recorded.

2.6. Continuous variation analysis (Job's plot)

Job's continuous variation method was employed to determine the binding stoichiometry by fluorescence spectroscopy [31,32]. At constant temperature, the fluorescence signal was recorded for solutions where the concentrations of both poly(A) and MB were varied while the sum of their concentration was kept constant at 50 μM. The difference in fluorescence intensity (ΔF) of MB at 685 nm in the absence and presence of poly(A) was plotted as a function of the input mol fraction of MB as reported previously [23,33]. The break point in the resulting plot corresponds to the mol fraction of the bound dye in the complex. The stoichiometry was obtained in terms of poly(A)-dye[$(1 - \chi_{dye})/\chi_{dye}$] where χ_{dye} denotes the mol fraction of the dye. The results presented are averages of at least three experiments.

2.7. Mode of binding: fluorescence quenching studies

Quenching studies were carried out with the anionic quencher potassium ferrocyanide. Two solutions, one KCl and the other $K_4[Fe(CN)_6]$, were mixed in different ratios to give a fixed total ionic strength. Fluorescence quenching experiments were performed at a constant P/D (RNA nucleotide phosphate/dye molar ratio) monitoring fluorescence intensity as a function of changing concentration of the ferrocyanide as described previously [34]. The data were plotted as Stern–Volmer plots of relative fluorescence intensity (F_o/F) versus $[Fe(CN)_6]^{4-}$.

2.8. Circular dichroism spectroscopy

Circular dichroism (CD) spectra were recorded on a PC controlled Jasco J815 unit (Jasco International Co. Ltd.,) equipped with a temperature controller and thermal programmer model PFD 425L/15 in rectangular quartz cuvettes of 1 cm path length at 20 ± 0.5 °C as reported earlier [28]. Each spectrum was averaged from at least five successive scans at a scan rate of 100 nm/min using a band width of 1 nm at a sensitivity of 100 milli degree, and was base line corrected and smoothed within permissible limits using the built-in Jasco software. The CD spectra were expressed as

molar ellipticity (θ) in terms of nucleotide phosphates versus wavelength. CD melting profiles were obtained by heating the sample (60.0 μM of poly(A) and 21 μM of MB) at a scan rate of 0.8 °C/min and monitoring the CD signal at 274 nm [23]. For the melting profiles, the ellipticity values are expressed in units of milli degrees. All CD measurements were repeated at least three times and the data are the average of these determinations.

2.9. Optical thermal melting studies

Absorbance versus temperature profiles (optical melting curves) of the complexes were measured on a Shimadzu Pharmaspec 1700 spectrophotometer equipped with a Peltier controlled TMSPC-8 model microcell accessory (Shimadzu Corporation, Kyoto, Japan), as reported previously [34]. In a typical melting experiment, poly(A) samples were mixed with the dye at appropriate ratio and diluted into the desired degassed buffer in the micro optical eight chambered cuvette of 1 cm light path length. The temperature of the microcell accessory was raised at a heating rate of 0.5 °C/min continuously monitoring the absorbance change at 257 nm. Melting curves allowed the monitoring of the hyperchromic change and estimation of melting temperature, T_m, the midpoint of the hyperchromic transition.

2.10. Differential scanning calorimetry

To investigate the helix-coil transition, excess heat capacities as a function of temperature were measured on a Microcal VP-differential scanning calorimeter (DSC) (MicroCal, Inc., Northampton, MA, USA) as described previously [35,36]. In a series of DSC scans, both the cells were loaded with buffer solution, equilibrated at 35 °C for 15 min and scanned from 35 °C to 110 °C at a scan rate of 50 °C/h. The buffer scans were repeated till reproducible (noise specification < 0.5 μcal/°C and repeatability specification $<$ 1.3 μcal/°C) and on cooling, the sample cell was rinsed and loaded with poly(A) and then with the poly(A)-dye complex (dye/poly(A) molar ratio = 0.25) and scanned in the range 35–110 °C. Each experiment was repeated twice with separate fillings. The DSC thermograms of excess heat capacity versus temperature were analyzed using the Origin 7.0 software. The area under the experimental heat capacity (c_p^o) curve was used to determine the calorimetric transition enthalpy (ΔH_{cal}) given by the equation

$$H_{cal} = \int C_p dT \quad (2)$$

where T is the absolute scale temperature in Kelvin. This calorimetrically determined enthalpy is model-independent and is thus unrelated to the nature of the transition. The temperature at which excess heat capacity is at a maximum defines the transition temperature (T_m). The model-dependent van't Hoff enthalpy (ΔH_v) was obtained by shape analysis of the calorimetric data and the cooperativity factor was obtained from the ratio ($\Delta H_{cal}/\Delta H_v$) [37].

2.11. Isothermal titration calorimetry

All isothermal titration calorimetry experiments were performed using a MicroCal VP-ITC unit (MicroCal, Inc., Northampton, MA, USA) at 20 °C as reported previously [23,33,36]. Aliquots of degassed MB solution were injected from a rotating syringe (290 rpm) into the isothermal sample chamber containing the poly(A) solution. Corresponding control experiments to determine the heat of dilution of MB were performed by injecting identical volumes of the same into the buffer. The duration of each injection was 10 s and the delay time between each injection was 240 s. The initial delay before the first injection was 60 s. Each injection generated a heat burst curve (microcalories per second versus time). The area under each heat burst curve was determined by integration using the Origin 7.0 software (MicroCal) to give the measure of the heat associated with that injection. The heat associated with each MB-buffer mixing was subtracted from the corresponding heat associated with the dye injection to the poly(A) to give the heat of dye binding to poly(A). The heat of dilution of injecting the buffer into the poly(A) solution was observed to be negligible. The resulting corrected injection heats were plotted as a function of the D/P [dye]/[nucleotide phosphate molar ratio], fit with a model for one set of binding sites, and analyzed using Origin 7.0 software to estimate the binding affinity (K_a), the binding stoichiometry (N) and the enthalpy of binding (ΔH^o). The free energies (ΔG^o) were calculated using the standard relationship

$$\Delta G^o = -RT\ln(K_a) \quad (3)$$

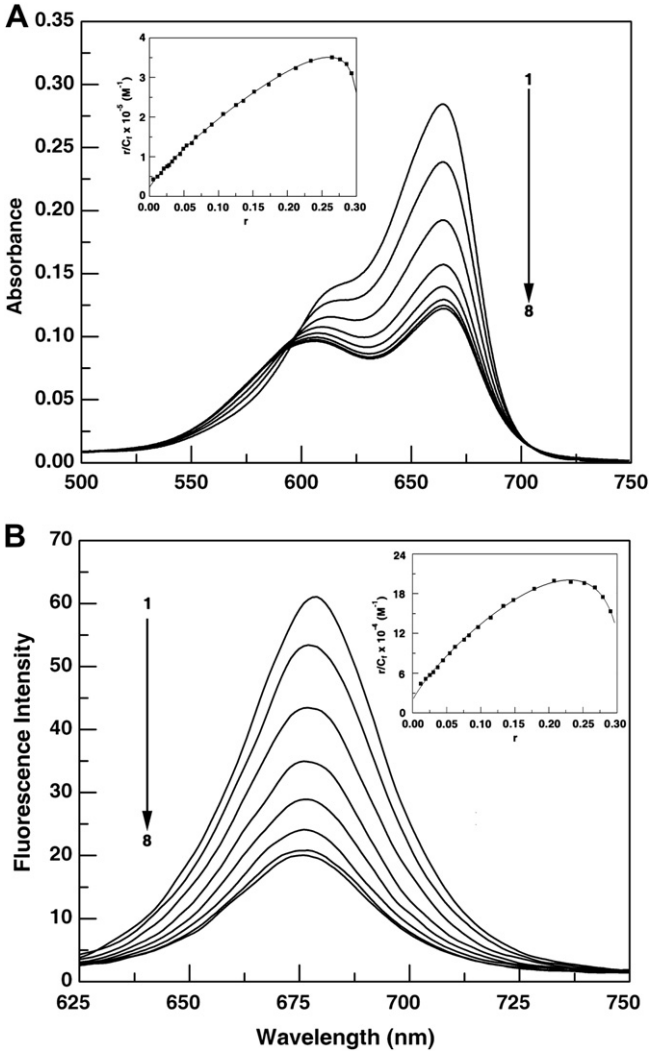

Fig. 2. (A) Representative absorption spectral changes of methylene blue (2.5 μM) treated with 0, 1.25, 3.75, 6.25, 7.50, 8.75, 10.0 and 12.5 μM (curves 1–8) of poly(A) in 100 mM CP buffer, pH 7.0 at 20 ± 0.5 °C. Inset: Cooperative Scatchard plot of methylene blue–poly(A) complexation obtained from spectrophotometric titration data. (B) Representative fluorescence emission spectral changes resulting on the interaction of methylene blue (5.0 μM) treated with 0, 1.25, 2.5, 5.0, 7.5, 10.0, 12.5, 15.0 μM (curves 1–8) of poly(A) in 100 mM CP buffer, pH 7.0 at 20 ± 0.5 °C. Inset: Cooperative binding profile of methylene blue–poly(A) complexation obtained from fluorescence titration data.

Table 1
Summary of optical properties of free and poly(A) bound methylene blue.[a]

Absorbance	
λ_{max} (free)	664, 612
λ_{max} (bound)	664
λ_{iso}[b]	594
ε_f (at λ_{max})	76,000 (664 nm)
ε_b (at λ_{max})	52,445
ε_{iso} (at λ_{iso})	53,975
Fluorescence	
λ_{max} (excitation)	610
λ_{max} (emission)	685
F_b/F_o[c]	0.30

[a] Units: λ nm; ε (molar extinction coefficient) M^{-1} cm^{-1}.
[b] Wavelength at the isosbestic points.
[c] F_o and F_b are the fluorescence intensities of the free and completely bound dye at 685 nm.

where R is the gas constant (1.987 cal. K^{-1} mol^{-1}) and T is the temperature in Kelvin (293.15 K). The binding free energy coupled with the binding enthalpy derived from the ITC data allowed the calculation of the entropic contribution ($T\Delta S^o$) to the binding, where ΔS^o is the calculated binding entropy using the standard relationship

$$T\Delta S^o = \Delta H^o - \Delta G^o \quad (4)$$

3. Results and discussion

3.1. Spectroscopic results and evaluation of binding affinity

In the 500–750 nm region of the visible absorption, MB has characteristic absorption spectrum with a peak around 664 nm and a shoulder around 612 nm [5,6]. The changes in the absorption spectrum may be conveniently used to monitor the interaction with poly(A). In Fig. 2A, the absorption spectral changes in MB on titration with increasing concentrations of poly(A) are presented. The spectrum marked '1' is the absorption spectrum of free MB molecule that underwent hypochromic and bathochromic effects on titration with increasing P/D (nucleotide phosphate/dye molar ratio) and a slight bathochromic shift of 2–3 nm with an isosbestic point at 594 nm. At saturating P/D, the change in hypochromicity of the 664 nm band was about 21%.

MB is a strongly fluorescent molecule. Its emission spectrum is in the 600–750 nm with maximum around 685 nm when excited at 610 nm. Complex formation was monitored by titration studies keeping a constant concentration of the dye and increasing the concentration of poly(A). With increasing concentration of poly(A), progressive quenching of the fluorescence of MB was observed eventually reaching a saturation point without any shift in the wavelength maximum (Fig. 2B). The optical properties of free and poly(A) bound MB molecules are presented in Table 1.

The results of the spectrophotometric and fluorimetric titrations were analyzed by constructing Scatchard plots. The Scatchard plots (inset of Fig. 2) exhibited cooperative behavior as revealed by positive slope at low r values and hence were analyzed further by the McGhee–von Hippel methodology [29] for cooperative binding

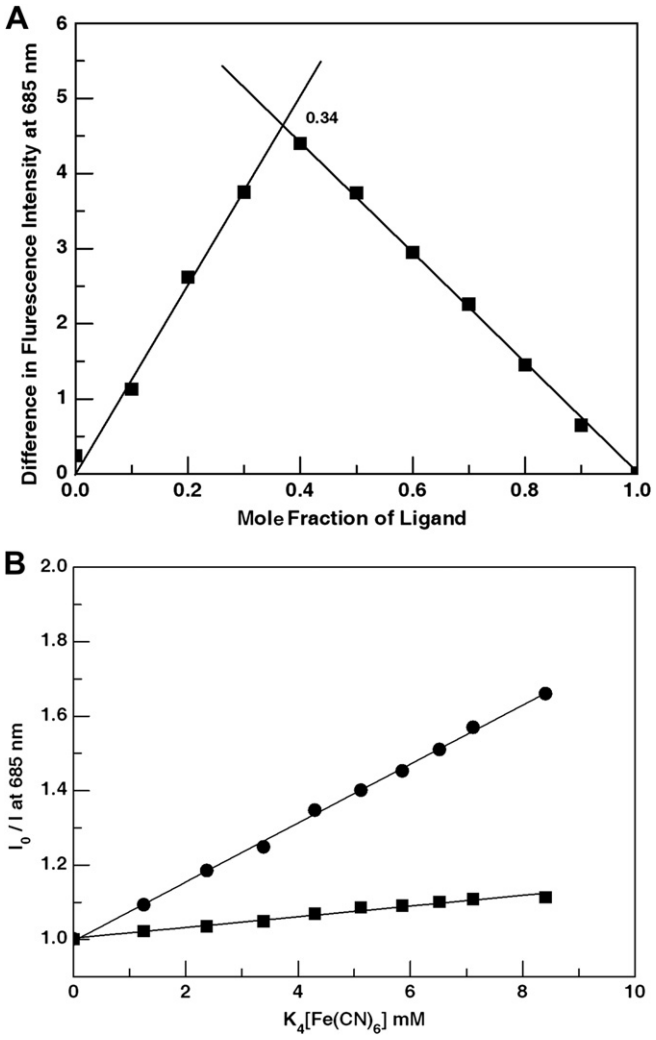

Fig. 3. (A) Job plot for methylene blue–poly(A) complexation in 100 mM CP buffer, pH 7.0 at 20 ± 0.5 °C. (B) Stern–Volmer plots for the quenching of methylene blue fluorescence in the absence (●) and presence (■) of poly(A).

using equation (1) for the evaluation of the binding constants. The cooperative binding affinity of MB to poly(A) was evaluated to be 2.30×10^4 M^{-1} and 1.80×10^4 M^{-1}, respectively, from absorbance and fluorescence data. These values along with the number of binding sites and the cooperativity factor (ω) are depicted in Table 2. The apparent binding constant (K) which is a product of the cooperative binding affinity and the cooperative factor ($K_i\omega$) gave values of 1.51×10^6 M^{-1} and 1.02×10^6 M^{-1}, respectively, indicating high binding affinity (of the order of 10^6 M^{-1}) for MB to poly(A).

3.2. Stoichiometry of the association

The stoichiometry of the association was determined independently by continuous variation analysis of Job in fluorescence. The

Table 2
Binding constant of methylene blue–poly(A) association from spectroscopic data.[a]

Spectrophotometry				Spectrofluorimerty			
K_i ($\times 10^4$ M^{-1})	n	ω	K ($\times 10^6$ M^{-1})	K_i ($\times 10^4$ M^{-1})	n	ω	K ($\times 10^6$ M^{-1})
2.30 ± 0.06	3.26 ± 0.03	65.84 ± 1.78	1.51 ± 0.08	1.80 ± 0.06	3.17 ± 0.04	56.82 ± 1.72	1.02 ± 0.02

[a] Average of four determinations at 20 ± 0.5 °C in CP buffer of 100 mM [Na^+], pH 7.0. Binding constants (K_i) refer to values obtained from Scatchard plots through McGhee–von Hippel analysis. K is the product of K_i and the cooperativity factor ω.

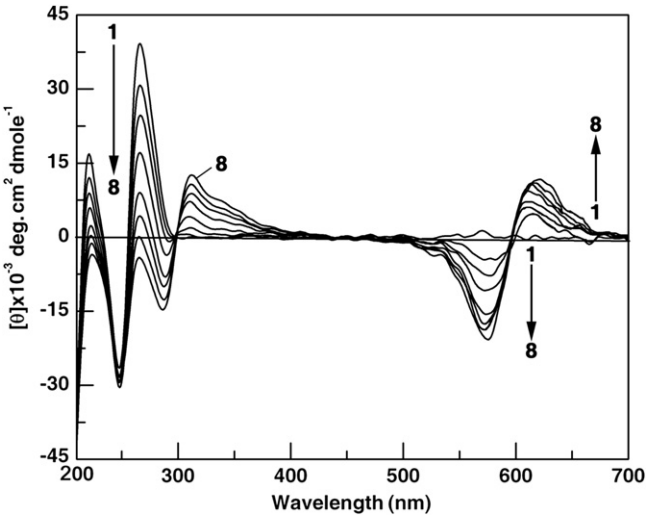

Fig. 4. Representative CD spectral changes resulting from poly(A) (60 μM) treated with 0, 30, 60, 90, 120, 150, 180, 210 μM (curves 1–8) of methylene blue in 100 mM CP buffer, pH 7.0 at 20 ± 0.5 °C.

plot of the difference in fluorescence intensity (ΔF) at 685 nm versus their mol fractions (Fig. 3A) revealed a single binding mode for MB on single stranded poly(A). From the inflection point, $\chi_{\text{MB-single stranded poly(A)}} = 0.34$ a value of 2.0 was estimated as the stoichiometry of the binding.

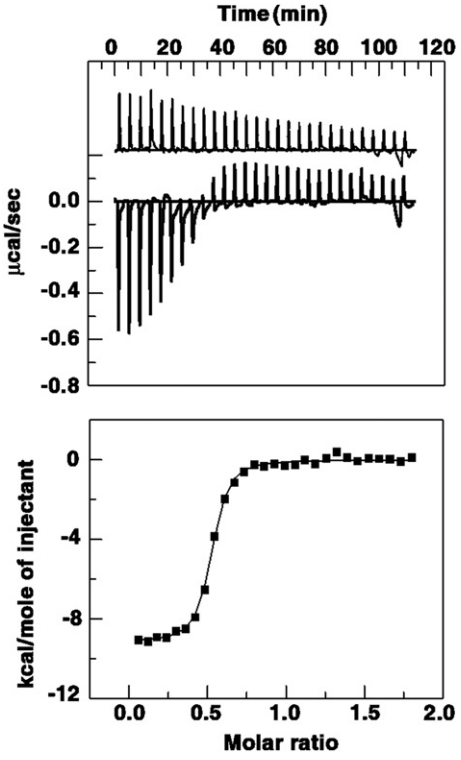

Fig. 5. Representative ITC profile for the titration of methylene blue (250 μM) with a solution of poly(A) (30 μM) in 100 mM CP buffer, pH 7.0 at 20 °C. In the top panel the heat burst curves are the result of successive injection of 10 μl aliquots of the dye into the poly(A). The bottom panel represents the corresponding normalized heat signals versus molar ratio. The control heat bursts of titration of the dye into buffer are presented in the top panel (curves offset of clarity).

Table 3
Thermodynamic parameters for the binding of MB to poly(A) in CP buffer pH 7.0 at different [Na^+] concentrations.[a]

[Na^+]	K_a ($\times 10^6$ M^{-1})	n	ΔG^o (kcal/mol)	ΔH^o (kcal/mol)	$T\Delta S^o$ (kcal/mol)
10	2.09 ± 0.40	1.70 ± 0.02	−8.47 ± 0.26	−9.84 ± 0.26	−1.36
50	2.79 ± 0.47	1.96 ± 0.01	−8.64 ± 0.16	−9.46 ± 0.16	−0.81
100	6.24 ± 0.60	1.98 ± 0.02	−9.12 ± 0.07	−9.00 ± 0.07	−0.12
200	7.23 ± 0.18	2.27 ± 0.03	−9.20 ± 0.09	−8.86 ± 0.09	−0.34

[a] The data in this table were derived from ITC experiments and are averages of four determinations at 20 °C. K_a and ΔH^o values were determined from ITC profiles fitting to Origin 7.0 software as described in the text. The values of ΔG^o and $T\Delta S^o$ were determined using equations $\Delta G^o = -RT\ln K_a$, and $T\Delta S^o = \Delta H^o - \Delta G^o$. All ITC profiles were fit to a model of single binding site.

3.3. Mode of binding: fluorescence quenching studies

For investigating the mode of binding of small molecules to nucleic acid structure fluorescence quenching experiments provide an effective method [34]. In the complex, molecules that are free or bound on the surface of the poly(A) may be readily available to an anionic quencher, while those that are inserted between bases/base

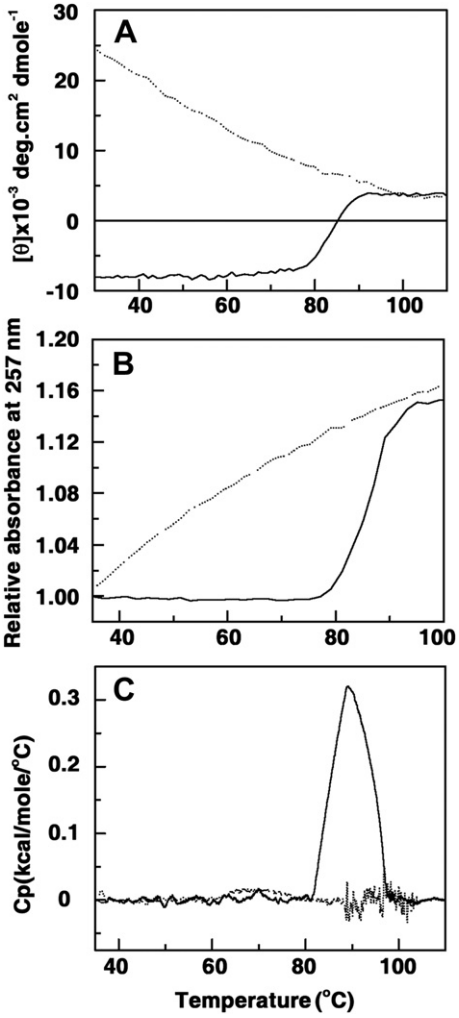

Fig. 6. (A) Circular dichroism melting profiles of poly(A) (…) and methylene blue–poly(A) complex (—) monitored at wavelength 275 nm. (B) Representative optical thermal melting profiles of poly(A) (…) and methylene blue–poly(A) complex (—) monitored at 260 nm. (C) DSC thermogram of poly(A) (…) and methylene blue–poly(A) complex (—), at 100 mM CP buffer, pH 7.0.

pairs of the polynucleotide may be inaccessible. The electrostatic barrier due to the negative charges on the phosphate groups at the helix surface limits the penetration of an anionic quencher into the interior of the helix. Hence, very little or no quenching may be observed in the presence of an anionic quencher, if the binding involves intercalation/strong stacking. Consequently the magnitude of the Stern–Volmer quenching constant (K_{sv}) of the ligands that are bound inside will be lower than that of the free molecules. It has been revealed that binding to the poly(A) resulted in decreased quenching of the fluorescence intensity of MB (Fig. 3B). K_{sv} values for free MB and its complex with poly(A) were 79.2 and 14.4 L/mol, respectively, indicating that the bound MB is less accessible to the quencher or in other words are considerably protected and sequestered away from the solvent suggesting intercalative binding with poly(A).

3.4. Circular dichroism studies

Conformational changes associated with the binding of MB with single stranded poly(A) were probed through circular dichroism studies. Poly(A) has a characteristic CD spectrum with a large positive band around 265 nm and a less intense negative band around 248 nm (curve 1 in Fig. 4). CD spectral changes accompanying the interaction of MB with poly(A) were characterized by a decrease in the positive peak at 265 nm with no change in the negative CD ellipticity. The formation of induced CD bands with enhancing ellipticity as the binding progressed, was also visible (Fig. 4). The series of spectra revealed two induced positive cotton couplets. The one in the 550–620 nm may be considered to arise from the coupling of the transition moments of the intercalated methylene blue having a clockwise disposition of their transition moments in the double helical poly(A). A couplet of similar intensity appears in the 300–400 nm region also. The presence of isodichroic points in the series of spectra suggests that the bound and free molecules are in equilibrium as revealed from absorption spectral studies also.

3.5. Isothermal titration calorimetry

To characterize the energetics of the binding of MB to the single stranded poly(A) isothermal titration calorimetry experiments were performed. ITC is an important and reliable tool for the direct measurement of thermodynamic parameters in various biological interactions [37]. In Fig. 5 (upper panel) the representative raw ITC profiles resulting from the titration of poly(A) to MB solution is presented. Each of the heat burst curves in the figure corresponds to a single injection. The areas under these heat burst curves were determined by integration to yield the associated injection heats. These injection heats were corrected by subtracting the corresponding dilution heats derived from the injection of identical amounts of the injectant, MB, into the buffer alone (curves in the upper panel offset for clarity). In the lower panel of the figure, the resulting corrected injection heats are plotted against the respective molar ratios. In this panel the data points reflect the experimental injection heat while the solid lines reflect calculated fits of data. The corrected isotherms obtained at 20 °C showed a single site binding event indicating that only one type of complex was formed, thus enabling the fitting to a single site protocol in ITC. The binding affinity and the other thermodynamic parameters of MB to poly(A) are presented in Table 3.

The affinity of MB to poly(A) at 100 mM was very high at 6.24×10^6 M^{-1}. This is much higher than the values of binding constant reported for DNA in the literature [3–6]. The slightly higher value of K obtained here compared to that in spectroscopy indicates the higher accuracy of the ITC technique. The data revealed that the free energy of the binding to be −9.12 kcal/mol. The small entropy term (−0.12 kcal/mol) and the large enthalpy contribution (−9.19 kcal/mol) revealed that the binding was purely

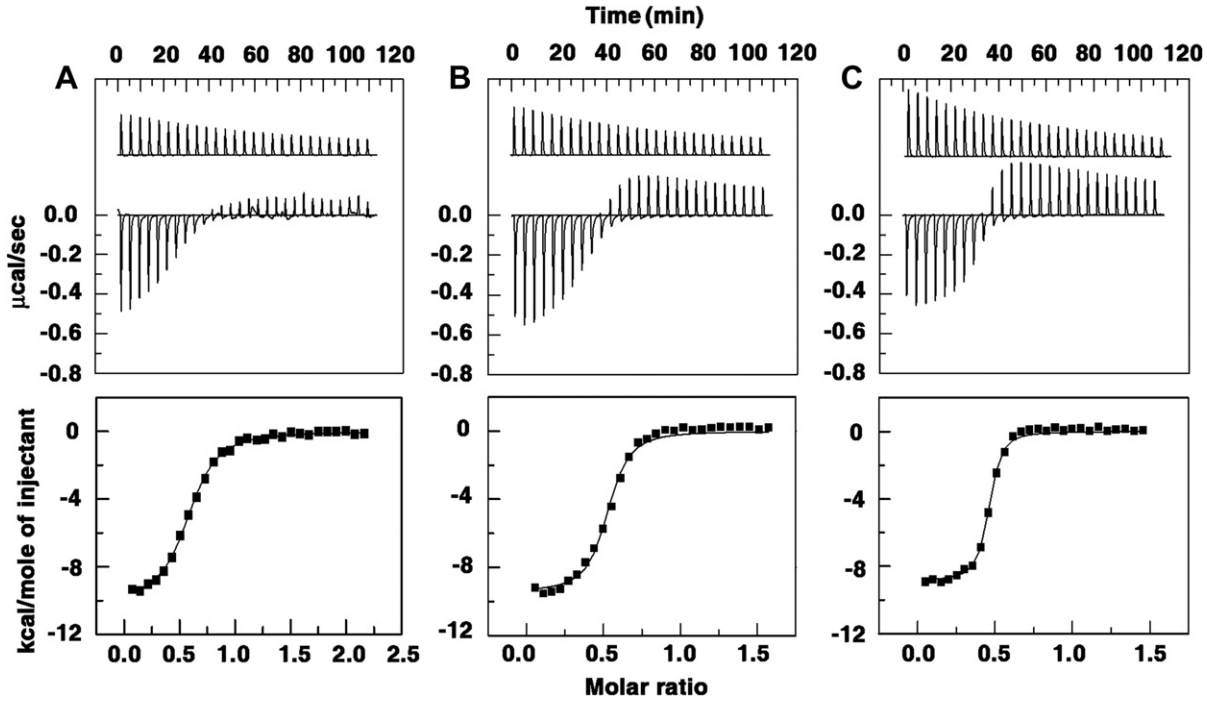

Fig. 7. Representative ITC profiles for the titration of (A) methylene blue (200 µM) into a 20 µM solution of poly(A) 10 mM [Na^+] (B) methylene blue (280 µM) into a 37 µM solution of poly(A) 50 mM [Na^+] (C) methylene blue (280 µM) into a 40 µM solution of poly(A) in 200 mM [Na^+] CP buffer at pH 7.0 at 20 °C. In the top panel each heat burst curve is the result of the injection of 10 µl of the ligand in to the poly(A) solution. The bottom panel represents the corresponding normalized heat signals versus molar ratio. The control heat bursts of titration of the dye into buffer are presented in the top panel (curves offset of clarity).

enthalpy driven. The binding was exothermic and the stoichiometry was found to be 2 mol of ligand binding per mole of poly(A). These values are in good agreement with the values obtained from Job plot analysis.

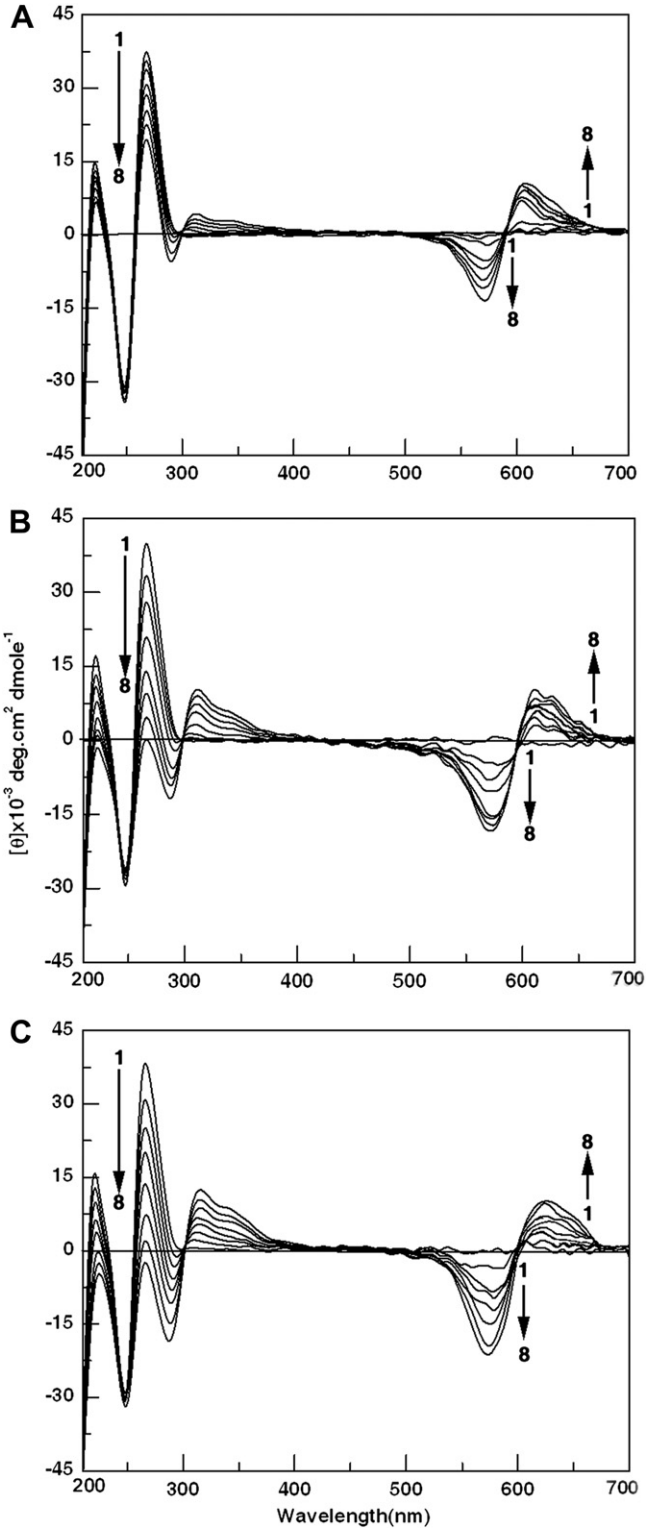

Fig. 8. Representative CD spectra resulting from interaction of poly(A) (60 μM) treated with 0, 30, 60, 90, 120, 150, 180, 210 μM (curves 1–8) of methylene blue in (A) 10 mM [Na^+] (B) 50 mM [Na^+] (C) 200 mM [Na^+] CP buffer, pH 7.0 at 20 ± 0.5 °C.

3.6. Self-assembled structure formation in poly(A)

Self-assembled structure formation is an important recently revealed aspect of many small molecule-poly(A) interactions [15,16,22,23,38]. One of our aims in this study was to investigate the capability of MB in inducing self-assembly in single stranded poly(A) and this was investigated from CD melting and UV melting and differential scanning calorimetric studies (Fig. 6). We found cooperative melting of poly(A)-MB complex in CD (Fig. 6A) and optical melting (Fig. 6B) studies indicating the formation of self-assembled structure in poly(A). The melting temperature of this self structured poly(A)-MB complex was around 86 °C. Furthermore, the DSC thermogram (Fig. 6C) indicated a remarkably strong peak with T_m around 87 °C compared to a flat thermogram for poly(A) alone proving unequivocally the formation of self-assembly structure. Furthermore, the values of ΔH_{cal} and $\Delta H_{vant\ Hoff}$ are identical (~10.06 kcal/mol) for the complex as revealed from the DSC data suggesting a truly cooperative reversible transition for the MB-poly(A) structure. Self-assembled structure induction in poly(A) by planar molecules has been supported by intercalative geometry and the melting results confirm such helical organization induced by methylene blue.

3.7. Salt dependent ITC and CD studies: role of electrostatic interaction

MB is a cationic dye with a positive charge on its conjugated ring system. To understand the role of electrostatic interaction in the binding process, salt dependence of the binding of MB with single stranded poly(A) was performed by ITC and CD experiments at three [Na^+] concentrations viz. 10, 50 and 200 mM in addition to that performed at 100 nm. The results are presented in Fig. 7 and the thermodynamic parameters elucidated are depicted in Table 3. The binding constant moderately increased as the salt concentration increased in the range 10–50 mM and raised remarkably in the range 50–100 nm. Earlier studies on the interaction of MB with single and double stranded DNA have reported that the salt increase decreased the binding affinity due to the shielding of the electrostatic charges [5,6,13,39]. We have observed that below 50 mM of [Na^+] no self-assembled structure was formed in poly(A) in presence of MB. Thus, shielding of the electrostatic charges in poly(A) appears to favor the self-assembled structure formation and hence the binding affinity increases due to favorable intercalation on to the duplex poly(A). An increase in the binding affinity of berberine was previously reported by Yadav et al. [40] which again is possibly due to self-assembled structure formation that was subsequently demonstrated with berberine [41,42].

The CD spectral changes of the interaction were also followed at three salt concentrations other than 100 mM to complement the observed increase in binding as the salt increased. The data is presented in Fig. 8. It can be seen that the conformational changes in poly(A) were more pronounced as the salt concentration enhanced. This was also complemented by the higher intensity for the induced CD bands of methylene blue in the complex. This result confirms that the binding was favored at higher salt concentration probably due to the ease of formation of self-assembled structure.

4. Conclusions

The present study reveals that the phenothiazinium dye methylene blue binds strongly with affinity of the order of $10^6\ M^{-1}$ to single stranded poly(A). Two induced CD patterns revealed strong chiral orientation of the bound methylene blue on the poly(A). Calorimetric studies revealed that the binding was enthalpy driven and the binding affinity enhanced with salt concentration in the

range 10–200 mM [Na^+]. This was also revealed and confirmed from the circular dichroism spectral data and the ellipticity of the induced circular dichroism bands. Binding leads to conformational rearrangement in poly(A) leading to self-assembled structure formation that was favored as the salt concentration enhanced.

Acknowledgments

This work was supported by grants from the network project entitled "*Comparative genomics and biology of noncoding RNA in the human genome*" (NWP0036) of the Council of Scientific and Industrial Research (CSIR), Government of India. Dr. Maidul Hossain is supported by the Research Associateship of the CSIR. Ayesha Kabir is a recipient of the NET-Junior Research Fellowship of the CSIR. The authors gratefully acknowledge the help and cooperation of all the members of the Biophysical Chemistry Laboratory at every stage of this work. We appreciate the critical and judicious comments of the two anonymous reviewers that helped us to improve the manuscript.

References

[1] Tuite EM, Kelly JM. Photochemical interactions of methylene blue and analogues with DNA and other biological substrates. J Photochem Photobiol B Biol 1993;21:103–24.
[2] Tuite EM, Norden B. Sequence specific interactions of methylene blue with polynucleotides and DNA: a spectroscopic study. J Am Chem Soc 1994;116:7548–56.
[3] Zhang LZ, Tang GQ. The binding properties of the photosensitizer methylene blue to herring sperm DNA: a spectroscopic study. J Photochem Photobiol B Biol 2004;74:119–25.
[4] Fujimoto BS, Clendenning JB, Delrow JJ, Heath PJ, Schurr M. Fluorescence, photo bleaching studies of methylene blue binding to DNA. J Phys Chem 1994;98:6633–43.
[5] Hossain M, Giri P, Suresh Kumar G. DNA intercalation by quinacrine and methylene blue: a comparative binding and thermodynamic characterization study. DNA Cell Biol 2008;27:81–90.
[6] Hossain M, Suresh Kumar G. DNA intercalation of methylene blue and quinacrine: new insights into base and sequence specificity from structural and thermodynamic studies. Mol BioSyst 2009;5:1311–22.
[7] McBride TJ, Schneider JE, Floyd RA, Loeb LA. Mutations induced by methylene blue plus light in single-stranded M13mp2. Proc Natl Acad Sci USA 1992;89:6866–70.
[8] Pádula M, Boiteux S. Photodynamic DNA damage induced by phycocyanin and its repair in *Saccharomyces cerevisiae*. Braz J Med Biol Res 1999;32:1063–71.
[9] Severino D, Junqueira HC, Gugliotti M, Gabrielli DS, Baptista MS. Influence of negatively charged interfaces on the ground and excited state properties of methylene blue. Photochem Photobiol 2003;77:459–68.
[10] Gabrielli D, Belisle E, Severino D, Kowaltowski AJ, Baptista MS. Binding, aggregation and photochemical properties of methylene blue in mitochondrial suspensions. Photochem Photobiol 2004;79:227–32.
[11] Malins DC, Polissar NL, Ostrander GK, Vinson MA. Single 8-oxo-guanine and 8-oxo-adenine lesions induced marked changes in the backbone structure of a 25-base DNA strand. Proc Natl Acad Sci USA 2000;97:12442–5.
[12] Sies H, Menck CFM. Singlet oxygen-induced DNA damage. Mutat Res 1992;275:367–75.
[13] Ortiz M, Fragoso A, Ortiz PJ, O'Sullivan CK. Elucidation of the mechanism of single-stranded DNA interaction with methylene blue: a spectroscopic approach. J Photochem Photobiol A Chem 2011;218:26–32.
[14] Harford JB. Translation-targeted therapeutics for viral diseases. Gene Expr 1995;4:357–67.
[15] Giri P, Suresh Kumar G. Molecular aspects of small molecules-poly(A) interaction: an approach to RNA based drug design. Curr Med Chem 2009;16:965–87.
[16] Giri P, Suresh Kumar G. Molecular recognition of poly(A) targeting by protoberberine alkaloids: in vitro biophysical studies and biological perspectives. Mol BioSyst 2010;6:81–8.
[17] Wickens M, Anderson P, Jackson RJ. Life and death in the cytoplasm: messages from the 3′ end. Curr Opin Genet Dev 1997;7:220–32.
[18] Dower K, Kuperwasser N, Merrikh H, Rosbash M. A synthetic A tail rescues yeast nuclear accumulation of ribozyme-terminated transcript. RNA 2004;10:1888–99.
[19] Saenger W. Principles of nucleic acid structure. New York: Springer-Verlag; 1984.
[20] Petrovic AG, Polavarapu PL. Structural transitions in polyriboadenylic acid induced by the changes in pH and temperature: vibrational circular dichroism study in solution and film states. J Phys Chem B 2005;109:23698–705.
[21] Scovell WM. Structural and conformational studies of polyriboadenylic acid in neutral and acid solution. Biopolymers 1978;17:969–84.
[22] Giri P, Suresh Kumar G. Isoquinoline alkaloids and their binding with polyadenylic acid: potential basis of therapeutic action. Mini-Rev Med Chem 2010;10:568–77.
[23] Giri P, Suresh Kumar G. Self-structure induction in single stranded poly(A) by small molecules: studies on DNA intercalators, partial intercalators and groove binding molecules. Arch Biochem Biophys 2008;474:183–92.
[24] Zarudnaya MI, Hovorun DM. Structural transitions in polyadenylic acid and hypothesis on biological role of its double-stranded forms. Ukr Biokhim Zh 1999;71:15–20.
[25] Zarudnaya MI, Hovorun DM. Hypothetical double-helical poly(A) formation in a cell and its possible biological significance. IUBMB Life 1999;48:581–4.
[26] Ciatto C, D'Amico ML, Natile G, Secco F, Venturini M. Intercalation of proflavine and a platinum derivative of proflavine into double-helical poly(A). Biophys J 1999;77:2717–24.
[27] Bergmann K, O'Konski CT. A spectroscopic study of methylene blue monomer, dimer, and complexes with montmorillonite. J Phys Chem 1963;67:2169–77.
[28] Bhadra K, Maiti M, Suresh Kumar G. Molecular recognition of DNA by small molecules: aT base pair specific intercalative binding of cytotoxic plant alkaloid palmatine. Biochim Biophys Acta 2007;1770:1071–80.
[29] McGhee JD, von Hippel PH. Theoretical aspects of DNA-protein interactions: co-operative and non-co-operative binding of large ligands to a one-dimensional homogeneous lattice. J Mol Biol 1974;86:469–89.
[30] Sinha R, Islam MM, Bhadra K, Suresh Kumar G, Banerjee A, Maiti M. The binding of DNA intercalating and non-intercalating compounds to A-form and protonated form of poly (rC)· poly (rG): spectroscopic and viscometric study. Bioorg Med Chem 2006;14:800–14.
[31] Job P. Formation and stability of inorganic complexes in solution. Ann Chim 1928;9:113–203.
[32] Huang CY. Determination of binding stoichiometry by the continuous variation method: the Job plot. In: Colowick SP, Kaplan NO, editors. Methods enzymol, vol. 87. Academic Press; 1982. p. 509–25.
[33] Giri P, Suresh Kumar G. Specific binding and self-structure induction to poly(A) by the cytotoxic plant alkaloid sanguinarine. Biochim Biophys Acta 2007;1770:1419–26.
[34] Das S, Suresh Kumar G. Molecular aspects on the interaction of phenosafranine to deoxyribonucleic acid: model for intercalative drug–DNA binding. J Mol Struct 2008;872:56–63.
[35] Islam MM, Sinha R, Suresh Kumar G. RNA binding small molecules: studies on t-RNA binding by cytotoxic plant alkaloids berberine, palmatine and the comparison to ethidium. Biophys Chem 2007;125:508–20.
[36] Giri P, Suresh Kumar G. Spectroscopic and calorimetric studies on the binding of the phototoxic and cytotoxic plant alkaloid sanguinarine with double helical poly(A). J Photochem Photobiol A Chem 2008;194:111–21.
[37] Haq I, Chowdhry BZ, Jenkins TC. Calorimetric techniques in the study of high order DNA-drug interactions. In: Chaires JB, Waring MJ, editors. Methods enzymol, vol. 340. Academic Press; 2001. p. 109–49.
[38] Xing F, Song G, Ren J, Chaires JB, Qu X. Molecular recognition of nucleic acids: coralyne binds strongly to poly (A). FEBS Lett 2005;579:5035–9.
[39] Mudasir, Wahyuni ET, Tjahjono DH, Yoshioka N, Inoue H. Spectroscopic studies on the thermodynamic and thermal denaturation of the ct-DNA binding methylene blue. Spectrochim Acta A Mol Biomol Spectrosc 2010;77:528–34.
[40] Yadav RC, Suresh Kumar G, Bhadra K, Giri P, Sinha R, Pal S, et al. Berberine, a strong polyriboadenylic acid binding plant alkaloid: spectroscopic, viscometric, and thermodynamic study. Bioorg Med Chem 2005;13:165–74.
[41] Centikol OP, Hud NV. Molecular recognition of poly (A) by small ligands: an alternative method of analysis reveals nanomolar, cooperative and shape-selective binding. Nucleic Acids Res 2009;37:611–21.
[42] Islam MM, Basu A, Suresh Kumar G. Binding of 9-*O*-(ω-amino) alkyl ether analogues of the plant alkaloid berberine to poly(A): insights into self-structure induction. Med Chem Comm 2011;2:631–7.